

Self-Certifying Primal-Dual Optimization Proxies for Large-Scale Batch Economic Dispatch

Michael Klamkin, Mathieu Tanneau, Pascal Van Hentenryck

NSF AI Institute for Advances in Optimization

Georgia Institute of Technology, Atlanta, GA, United States

Abstract—Recent research has shown that optimization proxies can be trained to high fidelity, achieving average optimality gaps under 1% for large-scale problems. However, worst-case analyses show that there exist in-distribution queries that result in orders of magnitude higher optimality gap, making it difficult to trust the predictions in practice. This paper aims at striking a balance between classical solvers and optimization proxies in order to enable *trustworthy deployments with interpretable speed-optimality tradeoffs based on a user-defined optimality threshold*. To this end, the paper proposes a hybrid solver that leverages duality theory to efficiently bound the optimality gap of predictions, falling back to a classical solver for queries where optimality cannot be certified. To improve the achieved speedup of the hybrid solver, the paper proposes an alternative training procedure that combines the primal and dual proxy training. Experiments on large-scale transmission systems show that the hybrid solver is highly scalable. The proposed hybrid solver achieves speedups of over 1000x compared to a parallelized simplex-based solver while guaranteeing a maximum optimality gap of 2%.

Index Terms—deep learning, economic dispatch, optimization proxies

I. INTRODUCTION

In order to plan and operate modern power grids, Transmission Systems Operators (TSOs) regularly have to solve large numbers of parametric optimization problems, e.g., multi-year simulations for transmission and capacity planning [1], or Monte-Carlo simulations for short-term risk analysis [2, 3]. Parametric optimization problems also appear in stochastic optimization formulations, which have received growing interest as renewable generation and distributed energy resources are integrated into the grid [4, 5].

The computational cost of solving large batches of similar instances (in the tens or hundreds of thousands) has fueled significant interest in *optimization proxies*, Machine Learning-based (ML) surrogate models that emulate the behavior of optimization solvers. Once trained, optimization proxies can produce close-to-optimal solutions to large-scale problems in milliseconds [6, 7]. Nevertheless, although proxies enjoy inference speeds that are orders of magnitude faster than classical optimization algorithms, their lack of strong worst-case performance guarantees has hindered their widespread adoption in real-life settings.

To address this limitation, the paper proposes a hybrid solver framework that, for the first time, combines the speed of data-

driven proxies with the worst-case guarantees of optimization solvers. A core component of this framework is to jointly learn primal *and* dual feasible solutions, thus providing a self-contained mathematical certificate of performance in the form of a provable duality gap. This unique self-certifying capability enables the systematic detection of poor predictions *online*, without ground truth information. Namely, when the duality gap of a predicted primal-dual solution exceeds a user-prescribed optimality tolerance, the corresponding instance is solved exactly using a classical optimization solver. This strategy ensures worst-case optimality guarantees while providing a large overall speedup since, in practice, only a small fraction of samples exhibit poor performance. In addition, it provides an interpretable way to tradeoff optimality and speedup.

A. Related Works

1) *Optimization Proxies*: Recent research has explored how to design *feasible* optimization proxies: architectures that guarantee by construction the feasibility of the solution [8–13]. In particular, Chen et al. [10] proposes a differentiable repair layer based on proportional response to efficiently produce primal-feasible solutions to the economic dispatch problem. Nevertheless, despite substantial progress on the theory and practice of optimization proxies, their widespread adoption remains hindered by their lack of worst-case performance guarantees. Indeed, Chen et al. [14] show that, while proxies may achieve low optimality gaps on average (e.g. under 1%), their worst-case performance can be orders of magnitude larger (e.g. above 100%), well beyond practically reasonable tolerances.

2) *Neural Network Verification*: In order to enable responsible adoption of proxies in practice, recent work has began to consider how to bound the sub-optimality of trained proxies by adapting techniques from neural network verification (NNV) [15]. Nellikkath and Chatzivasileiadis [16] applies MIP reformulation techniques for verifying the worst-case infeasibility of ACOPF proxies. Nellikkath et al. [17] proposes primal acceleration techniques, using state-of-the-art NNV solvers [18] for verifying DCOPF proxies. Chen et al. [14] considers primal-feasible proxies for economic dispatch, proposing a first-order method to approximate the worst-case sub-optimality.

It is important to note that [14, 16, 17] all show that worst-case performance in trained optimization proxies is often orders of magnitude worse than average performance; in other

Submitted to the 24th Power Systems Computation Conference (PSCC 2026).

words, optimization proxies are not immune to adversarial attacks. Thus, relying on neural network verification tools as a screening procedure for proxy adoption, besides being computationally expensive, leads to overly pessimistic conclusions.

3) *ML-accelerated Optimization*: Another line of work considers warm-starting schemes, where machine learning predictions are used to set the initialization of a classical solver. Then, the overall scheme inherits both feasibility and optimality guarantees from the termination of the classical solver. Prior works in this direction report speedups on the order of 2-25x [19–22]. This paper strikes a balance between warm-starting and directly using predictions; it proposes a scheme that allows to avoid the solver entirely for a majority of queries, unlocking further speedup on the order of 1000x.

B. Contributions and Outline

The paper contributions are summarized as follows:

- 1) It introduces a principled hybrid solver framework that, for the first time, provides *controllable* worst-case optimality guarantees without 1) requiring any expensive offline verification step nor 2) imposing restrictions on the underlying architectures. Importantly, the optimality tolerance is prescribed by the user rather than being derived from properties of the underlying models.
- 2) It improves the training of primal-dual proxies by taking advantage of their self-certifying nature and uses a dedicated loss function.
- 3) It presents a complete implementation of the proposed framework for the economic dispatch problem and conducts extensive numerical experiments on large-scale instances based on the European transmission system.
- 4) It demonstrates state-of-the-art performance for solving large batches of industry-scale economic dispatch problems. On the 9241_pegase test case, the hybrid solver achieves up to 925x speedup over a parallelized simplex-based solver while guaranteeing worst-case optimality below 1%, and over 1000x at 2%.

The rest of the paper is organized as follows: Section II proposes the hybrid solver framework, Section III describes the proposed training algorithm, Section IV presents the numerical experiments, and Section V concludes the paper.

II. SELF-CERTIFYING PROXIES

This section introduces the notations used throughout the paper by reviewing linear programming, duality, and optimization proxies. Then, it presents the hybrid solver, which exploits the self-certifying property of primal-dual feasible solutions.

A. Linear Programming and Duality

For ease of reading, the proposed framework is stated for general linear programming (LP) problems. Namely, consider a parametric LP problem in primal-dual form

$$P_\theta : \min_{\mathbf{x}} \{c_\theta^\top \mathbf{x} \mid A_\theta \mathbf{x} \geq b_\theta\}, \quad (1a)$$

$$D_\theta : \max_{\mathbf{y} \geq 0} \{b_\theta^\top \mathbf{y} \mid A_\theta^\top \mathbf{y} = c_\theta\}, \quad (1b)$$

where $\theta \in \mathbb{R}^p$ is the vector of parameters, which takes value in $\Theta \subseteq \mathbb{R}^p$, and $A_\theta \in \mathbb{R}^{m \times n}$, $b_\theta \in \mathbb{R}^m$ and $c_\theta \in \mathbb{R}^n$ are the (parametric) left-hand side matrix, right-hand side, and objective, respectively. For $\theta \in \Theta$, the primal and dual feasible sets are

$$\mathcal{X}_\theta = \{\mathbf{x} \in \mathbb{R}^n \mid A_\theta \mathbf{x} \geq b_\theta\}, \quad (2a)$$

$$\mathcal{Y}_\theta = \{\mathbf{y} \in \mathbb{R}^m \mid A_\theta^\top \mathbf{y} = c_\theta, \mathbf{y} \geq 0\}. \quad (2b)$$

The paper assumes that $\mathcal{X}_\theta \neq \emptyset$ and $\mathcal{Y}_\theta \neq \emptyset, \forall \theta \in \Theta$, i.e., the primal-dual feasible set is always non-empty. This mild technical assumption ensures that strong duality always holds.

The primal (resp. dual) objective value of a primal-feasible (resp. dual-feasible) solution $\mathbf{x} \in \mathcal{X}_\theta$ (resp. $\mathbf{y} \in \mathcal{Y}_\theta$) is denoted by $\phi_\theta(\mathbf{x}) = c_\theta^\top \mathbf{x}$ (resp. $\psi_\theta(\mathbf{y}) = b_\theta^\top \mathbf{y}$). The optimal value of P_θ (resp. D_θ) is denoted by ϕ_θ^* (resp. ψ_θ^*). Optimal solutions to the primal and dual problems are denoted by \mathbf{x}_θ^* and \mathbf{y}_θ^* . By LP duality, the primal- and dual-optimal values are equal, and any primal (resp. dual) feasible solution yields a valid upper (resp. lower) bound on the optimal value, i.e.,

$$\forall \theta \in \Theta, \forall (\mathbf{x}, \mathbf{y}) \in \mathcal{X}_\theta \times \mathcal{Y}_\theta, \psi_\theta(\mathbf{y}) \leq \psi^* = \phi^* \leq \phi_\theta(\mathbf{x}).$$

Finally, given $(\mathbf{x}, \mathbf{y}) \in \mathcal{X}_\theta \times \mathcal{Y}_\theta$, define the *duality gap*

$$\Gamma_\theta(\mathbf{x}, \mathbf{y}) = \phi_\theta(\mathbf{x}) - \psi_\theta(\mathbf{y}) \geq 0. \quad (3)$$

The duality gap provides a measure of how close to optimum a primal-dual solution is. Namely,

$$\Gamma_\theta(\mathbf{x}, \mathbf{y}) \geq \phi_\theta(\mathbf{x}) - \phi_\theta^* \geq 0, \quad (4a)$$

$$\Gamma_\theta(\mathbf{x}, \mathbf{y}) \geq \psi_\theta^* - \psi_\theta(\mathbf{y}) \geq 0. \quad (4b)$$

It is important to note that the duality gap only requires the knowledge of a primal-dual *feasible* solution, i.e., $\Gamma_\theta(\mathbf{x}, \mathbf{y})$ can be computed without knowing the problem's optimal value.

Remark: The LP setting is not a very restrictive assumption, as the proposed framework readily applies to nonlinear convex problems using conic duality. Readers are referred to [23] for a more detailed review of conic optimization and duality.

B. Hybrid Solver

The paper assumes access to primal and dual optimization proxies that produce primal and dual solutions, respectively. Formally, let p_α and d_β denote the primal and dual proxy models respectively, and let $\hat{\mathbf{x}} = p_\alpha(\theta)$ and $\hat{\mathbf{y}} = d_\beta(\theta)$ denote the predicted primal and dual solutions for parameter $\theta \in \Theta$. α (resp. β) refers to the primal (resp. dual) proxy's trainable parameters. It is further assumed that both proxies produce feasible solutions, i.e.,

$$\forall \theta \in \Theta, (p_\alpha(\theta), d_\beta(\theta)) \in \mathcal{X}_\theta \times \mathcal{Y}_\theta. \quad (5)$$

The assumption of primal-dual feasibility in Eq. (5) is not too restrictive. Indeed, state-of-the-art neural network architectures such as IIInet [24] or RAYEN [11] can impose arbitrary convex constraints on their outputs. In the specific case of economic dispatch problems, dedicated repair layers have been proposed that ensure primal feasibility [10]. In addition, Tanneau and Hentenryck [25] show how to build dual-feasible proxies for convex problems with bounded variables, which is the case

Algorithm 1 Hybrid solver inference

Input: query θ , optimality threshold ϵ
Output: feasible, ϵ -optimal prediction $(\tilde{\mathbf{x}}, \tilde{\mathbf{y}})$

```

1: Predict  $(\tilde{\mathbf{x}}, \tilde{\mathbf{y}}) \in \mathcal{X}_\theta \times \mathcal{Y}_\theta$ 
2: Compute  $\hat{g} = \Gamma_\theta(\tilde{\mathbf{x}}, \tilde{\mathbf{y}})$ 
3: if  $\hat{g} \leq \epsilon$  then
4:   return  $(\tilde{\mathbf{x}}, \tilde{\mathbf{y}})$ 
5: end if
6: return  $(\mathbf{x}_\theta^*, \mathbf{y}_\theta^*)$ 

```

for the economic dispatch problems considered in this work. Section IV-B presents the detailed architectures used for primal and dual proxies.

The proposed hybrid solver is presented in Algorithm 1. The solver takes as input the instance's parameter value θ and a user-defined optimality tolerance ϵ . First, a primal-dual solution $(\tilde{\mathbf{x}}, \tilde{\mathbf{y}})$ is predicted using the primal and dual proxies, whose duality gap \hat{g} is computed using (3). If the duality gap \hat{g} is below the optimality tolerance ϵ , the predicted solution $(\tilde{\mathbf{x}}, \tilde{\mathbf{y}})$ is returned. Otherwise, an optimal solution $(\mathbf{x}_\theta^*, \mathbf{y}_\theta^*)$ is computed using an optimization solver. Theorem 1 shows that the worst-case optimality gap is at most ϵ .

Theorem 1. Let $\theta \in \Theta$ and $\epsilon \geq 0$, and let $(\tilde{\mathbf{x}}, \tilde{\mathbf{y}})$ be the solution returned by Algorithm 1 with input θ, ϵ . The solution $(\tilde{\mathbf{x}}, \tilde{\mathbf{y}})$ is at most ϵ -suboptimal, i.e.,

$$\phi_\theta(\tilde{\mathbf{x}}) - \phi_\theta^* \leq \epsilon \quad \text{and} \quad \psi_\theta(\tilde{\mathbf{y}}) - \psi_\theta^* \leq \epsilon.$$

Proof. Note that $(\tilde{\mathbf{x}}, \tilde{\mathbf{y}})$ is always primal-dual feasible by construction. If $\hat{g} > \epsilon$, the result is immediate as $(\tilde{\mathbf{x}}, \tilde{\mathbf{y}})$ is optimal. If $\hat{g} \leq \epsilon$, recall that $(\tilde{\mathbf{x}}, \tilde{\mathbf{y}}) \in \mathcal{X}_\theta \times \mathcal{Y}_\theta$. The result is a direct consequence of (4). \square

It is important to note that the core enabler of the proposed framework is the availability of \hat{g} as a self-contained certificate of sub-optimality, by leveraging LP duality and the feasibility of the predicted solution $(\tilde{\mathbf{x}}, \tilde{\mathbf{y}})$. *This key result makes it possible to detect “bad” predictions online, without ground truth information, and call the optimization solver only when needed.* To the best of the authors' knowledge, this is the first data-driven hybrid framework that provides *controllable* worst-case optimality guarantees without any offline verification step.

III. JOINT PRIMAL-DUAL TRAINING

The standard self-supervised optimization proxy training performs empirical risk minimization (maximization) using the primal (dual) objective value [7]. Using a finite set of samples \mathcal{D} , the primal proxy training problem reads

$$\min_{\alpha} \quad \frac{1}{|\mathcal{D}|} \sum_{\theta \in \mathcal{D}} c_\theta^\top (p_\alpha(\theta)) \quad (6)$$

Optimization proxies are typically relatively small (under 10M parameters), making it tractable to train the primal and dual models in parallel, on a single consumer GPU even for large

scale power systems¹. Training the primal and dual models in parallel has several benefits, as discussed next. The parallel empirical risk minimization problem reads

$$\min_{\alpha, \beta} \quad \frac{1}{|\mathcal{D}|} \sum_{\theta \in \mathcal{D}} \Gamma_\theta(p_\alpha(\theta), d_\beta(\theta)) \quad (7)$$

where α and β represent the trainable parameters of the neural networks in the primal and dual optimization proxies respectively. Note that in terms of training gradients, the problem is totally separable in α and β . Furthermore, it recovers exactly the primal (dual)-only training problems due to the definition of Γ_θ .

A. Normalization

A key feature of the primal-dual setting is that it allows for principled normalization. Besides not relying on the optimal value, which is unknown at training and inference time, it is important that the normalization retains the self-certifying property – that the duality gap bounds from above the true optimality gaps – when such a guarantee is needed. In these cases, e.g. to implement Algorithm 1 for normalized optimality thresholds $\epsilon\%$, the predicted dual objective value is used, since it bounds from below the optimal value. This yields the (proper) normalized gap

$$\bar{\Gamma}_\theta(\mathbf{x}, \mathbf{y}) := \frac{\Gamma_\theta(\mathbf{x}, \mathbf{y})}{\psi_\theta(\mathbf{y})} \quad (8)$$

which bounds from above the ground truth optimality gaps of the primal and dual predictions, i.e. replacing Γ_θ with $\bar{\Gamma}_\theta$ in Step 2 of Algorithm 1 allows to certify

$$\frac{\phi_\theta(\mathbf{x}) - \phi_\theta^*}{\phi_\theta^*} \leq \epsilon\%, \quad \text{and} \quad \frac{\psi_\theta^* - \psi_\theta(\mathbf{y})}{\psi_\theta^*} \leq \epsilon\%.$$

In contexts where an exact bound on the true normalized optimality gap is not required, e.g. for normalizing the loss during training, estimates of the optimal value can be used. In particular, the experiments in Section IV-C normalize the training loss using the midpoint:

$$\tilde{\Gamma}_\theta(\mathbf{x}, \mathbf{y}) := \frac{\Gamma_\theta(\mathbf{x}, \mathbf{y})}{(\phi_\theta(\mathbf{x}) + \psi_\theta(\mathbf{y}))/2} \quad (9)$$

Note that the denominator is treated as a constant w.r.t. α and β when performing automatic differentiation during training, and validation metrics use the proper normalized gap (8).

B. Targeting an optimality tolerance

When jointly training primal-dual feasible optimization proxies for later use in a hybrid solver, practitioners often already have a target optimality threshold ϵ in mind. In this case, the following ReLU/hinge loss more directly optimizes the speedup of the hybrid solver:

$$\min_{\alpha, \beta} \quad \frac{1}{|\mathcal{D}|} \sum_{\theta \in \mathcal{D}} \Gamma_\theta^\epsilon \quad (10a)$$

$$\text{where} \quad \Gamma_\theta^\epsilon := \max(\Gamma_\theta(p_\alpha(\theta), d_\beta(\theta)) - \epsilon, 0) \quad (10b)$$

¹The largest case considered in the experiments, 9241_pegase, requires only 8GB of GPU memory for parallel training.

since it focuses on improving the proxies at points θ where $\Gamma_\theta(p_\alpha(\theta), d_\beta(\theta)) > \epsilon$, which would trigger the fallback to the classical solver in Algorithm 1. The experiments compare Γ^0 to $\Gamma^{1\%}$; note that Γ^0 recovers (7) due to (3).

C. Sampling without replacement

Optimization proxies are typically trained for thousands of epochs with $|\mathcal{D}|$ in the tens to hundreds of thousands [6], where one epoch corresponds to one “complete traversal” through \mathcal{D} ; in other words, each sample is seen many times during training. However, unlike the supervised learning setting where training data instances must be solved apriori – representing a considerable computational burden – in the self-supervised setting, generating new samples requires minimal computation. Thus, the paper proposes to *resample \mathcal{D} at each epoch so that each query is only seen once throughout training*.

This is equivalent to using a very large finite dataset, though can be implemented much more efficiently. In particular, the need for storage and CPU-GPU transfer of training data batches is eliminated since batches can be sampled on-demand, directly on the GPU. Although efficient and simple to implement, such implementations are uncommon due to the lack of a dependable convergence measure in the primal (dual)-only setting. Indeed, even self-supervised learning implementations are often based around finite datasets in order to leverage pre-computed optimal solutions to implement features such as performance-based dynamic scheduling of learning rate, checkpointing, and termination, necessitating labeling at least the validation set samples and increasing the overall training time. Training the primal and dual proxies jointly enables implementing these crucial features using reliable metrics based on the (normalized) duality gap, fully eliminating the requirement for labeled data to begin training. Importantly, this enables immediate and trustworthy (re-)training within larger workflows.

IV. NUMERICAL EXPERIMENTS

This section first describes the economic dispatch formulation used in this work as well as the architectures used to implement the primal and dual proxies. Then, experimental results are presented, using the hybrid solver framework to accelerate solving batches of economic dispatch instances on large-scale power system benchmarks 1354_pegase, 2869_pegase, and 9241_pegase from PGLib [26]. Summary statistics for each benchmark are included in Table II.

A. Economic Dispatch Formulation

Consider a power grid comprising N buses, E branches, D loads and G generators. The economic dispatch problem is

formulated as the parametric LP problem

$$\min_{\mathbf{p}^g, \mathbf{p}^f, \boldsymbol{\xi}} \quad c^\top \mathbf{p}^g + M e^\top \boldsymbol{\xi} \quad (11a)$$

$$\text{s.t.} \quad \Phi A_g \mathbf{p}^g - \mathbf{p}^f = \Phi A_d p^d \quad [\boldsymbol{\pi}] \quad (11b)$$

$$e^\top \mathbf{p}^g = e^\top p^d \quad [\boldsymbol{\lambda}] \quad (11c)$$

$$p \leq \mathbf{p}^g \leq \bar{p} \quad [\mathbf{z}, \bar{\mathbf{z}}] \quad (11d)$$

$$f - \boldsymbol{\xi} \leq \mathbf{p}^f \leq \bar{f} + \boldsymbol{\xi} \quad [\underline{\boldsymbol{\mu}}, \bar{\underline{\boldsymbol{\mu}}}] \quad (11e)$$

$$\boldsymbol{\xi} \geq 0 \quad [\mathbf{y}] \quad (11f)$$

parametrized by the vector of active power demands $p^d \in \mathbb{R}^D$. Decision variables $\mathbf{p}^g \in \mathbb{R}^G$, $\mathbf{p}^f \in \mathbb{R}^E$ and $\boldsymbol{\xi} \in \mathbb{R}^E$ denote active power dispatch, active power flow and line overflows, respectively. The notation e is used to denote an appropriately-sized vector whose entries are all equal to 1. The objective (11a) minimizes active power generation costs and thermal violation penalties, where M is a large positive constant, set to 150,000 in the experiments. Constraint (11b) expresses power flows using the network’s Power Transfer Distribution Factor (PTDF) matrix Φ and generator and load incidence matrices A_g and A_d . Constraint (11c) enforces global power balance. Constraints (11d) and (11e) enforce bounds on active power dispatch and power flows, respectively. Dual variables associated to each constraint are indicated between brackets. The dual of the economic dispatch reads

$$\max_{\boldsymbol{\lambda}, \boldsymbol{\pi}, \underline{\mathbf{z}}, \bar{\mathbf{z}}, \underline{\boldsymbol{\mu}}, \bar{\boldsymbol{\mu}}, \mathbf{y}} \quad \boldsymbol{\lambda} e^\top p^d + (\Phi A_d d)^\top \boldsymbol{\pi} + f^\top \underline{\boldsymbol{\mu}} - \bar{f}^\top \bar{\boldsymbol{\mu}} + p^\top \underline{\mathbf{z}} - \bar{p}^\top \bar{\mathbf{z}} \quad (12a)$$

$$\text{s.t.} \quad \boldsymbol{\lambda} e + (\Phi A_g)^\top \boldsymbol{\pi} + \underline{\mathbf{z}} - \bar{\mathbf{z}} = c \quad (12b)$$

$$- \boldsymbol{\pi} + \underline{\boldsymbol{\mu}} - \bar{\boldsymbol{\mu}} = 0 \quad (12c)$$

$$\underline{\boldsymbol{\mu}} + \bar{\boldsymbol{\mu}} + \mathbf{y} = M e \quad (12d)$$

$$\underline{\boldsymbol{\mu}}, \bar{\boldsymbol{\mu}}, \underline{\mathbf{z}}, \bar{\mathbf{z}}, \mathbf{y} \geq 0 \quad (12e)$$

To generate the training, validation, and testing samples, the PGLearn [27, Algorithm 1 and Table 1] method is used to sample p^d such that a wide range of total power demand is covered, including the challenging high-load regime. Note that unlike the PGLearn datasets, which include optimal solutions, as described in Section III-C the implementation in this paper does not collect solutions for training nor validation samples, allowing it to start training immediately.

To implement the CPU solver baseline as well as the fallback in Algorithm 1, a lazy constraint approach is used. Algorithm 2 describes the procedure, which is implemented in JuMP 1.28.0 [28] using the HiGHS 1.11.0 [29] solver. Using lazy constraints for the thermal limits drastically improves solve times; for 1354_pegase, Algorithm 2 is approximately 15x faster than an equivalent sparse phase-angle formulation, for 2869_pegase 45x faster, and for 9241_pegase 250x faster. Note that testing samples are solved individually offline to facilitate reporting results for different levels of ϵ , e.g. Figure 1. Furthermore, model building time is excluded from the solve time, and perfect sample-wise parallelism is emulated with 24 CPUs, i.e., the solve time for a batch of N samples each with

Algorithm 2 Lazy PTDF solver

Input: query p^d
Output: optimal solution $(\mathbf{p}^g, \mathbf{p}^f, \xi)$

```

1: Initialize  $\mathcal{C} \leftarrow \emptyset$ 
2: while true do
3:   Solve
      
$$\begin{aligned} \min_{\mathbf{p}^g, \mathbf{p}^f, \xi} \quad & c^\top \mathbf{p}^g + M e^\top \xi \\ \text{s.t.} \quad & (\Phi A_g \mathbf{p}^g)_i - \mathbf{p}_i^f = (\Phi A_d p^d)_i \quad \forall i \in \mathcal{C} \\ & (11c) - (11f) \end{aligned}$$

4:   Compute  $\tilde{\mathbf{p}}^f \leftarrow \Phi A_g \mathbf{p}^g - \Phi A_d p^d$ 
5:   Compute  $\xi = \max(\max(0, \tilde{\mathbf{p}}^f - \bar{f}), \max(0, \underline{f} - \tilde{\mathbf{p}}^f))$ 
6:   for each branch  $i$  in  $1:E$  do
7:     if  $\xi_i > 0$  and  $i \notin \mathcal{C}$  then
8:        $\mathcal{C} \leftarrow \mathcal{C} \cup \{i\}$            {add constraint  $i$ }
9:     end if
10:   end for
11:   if no constraints were added then
12:     return  $(\mathbf{p}^g, \tilde{\mathbf{p}}^f, \xi)$ 
13:   end if
14: end while

```

solve times t_i is computed using the ideal makespan bound $\max(\frac{1}{24} \sum_i t_i, \max_i(t_i))$.

B. Feasibility Guarantees

In order to guarantee the feasibility of the primal predictions, the experiments implement the following inference procedure, based on the proportional response layer [10]:

- 1) Predict $\tilde{\mathbf{p}}^g \in \{\mathbf{p}^g \mid \underline{p} \leq \mathbf{p}^g \leq \bar{p}\}$
- 2) Recover $\hat{\mathbf{p}}^g$ by using the proportional response layer [10, Eq. 4] to project $\tilde{\mathbf{p}}^g$ onto the hypersimplex $\{\mathbf{p}^g \mid e^\top \mathbf{p}^g = e^\top p^d, \underline{p} \leq \mathbf{p}^g \leq \bar{p}\}$, i.e.

$$\hat{\mathbf{p}}^g \leftarrow \begin{cases} (1 - \eta^\uparrow) \tilde{\mathbf{p}}^g + \eta^\uparrow \bar{p} & \text{if } e^\top \tilde{\mathbf{p}}^g < e^\top p^d \\ (1 - \eta^\downarrow) \tilde{\mathbf{p}}^g + \eta^\downarrow \underline{p} & \text{if } e^\top \tilde{\mathbf{p}}^g \geq e^\top p^d \end{cases}$$

$$\text{where } \eta^\uparrow := \frac{e^\top p^d - e^\top \tilde{\mathbf{p}}^g}{e^\top \bar{p} - e^\top \tilde{\mathbf{p}}^g} \text{ and } \eta^\downarrow := \frac{e^\top \tilde{\mathbf{p}}^g - e^\top p^d}{e^\top \bar{p} - e^\top \tilde{\mathbf{p}}^g}$$

- 3) Recover $\hat{\mathbf{p}}^f = \Phi A_g \hat{\mathbf{p}}^g - \Phi A_d p^d$.
- 4) Recover $\hat{\xi} = \max(\max(0, \hat{\mathbf{p}}^f - \bar{f}), \max(0, \underline{f} - \hat{\mathbf{p}}^f))$.

To guarantee dual-feasibility, the paper adopts Smoothed Self-Supervised Learning (S3L) [30], which for the economic dispatch reads:

- 1) Predict $\hat{\lambda} \in \mathbb{R}$ and $\hat{\pi} \in [-M, M]^E$
- 2) Recover $\underline{\mu} = \frac{\mu}{\bar{f} - \underline{f}} + \frac{\hat{\pi}}{2} + \sqrt{(\frac{\mu}{\bar{f} - \underline{f}})^2 + (\frac{\hat{\pi}}{2})^2}$
- 3) Recover $\hat{\mu} = \frac{\mu}{\bar{f} - \underline{f}} - \frac{\hat{\pi}}{2} + \sqrt{(\frac{\mu}{\bar{f} - \underline{f}})^2 + (\frac{\hat{\pi}}{2})^2}$
- 4) Compute $z = c - \hat{\lambda} e - (\Phi A_g)^\top \hat{\pi}$
- 5) Recover $\underline{\bar{z}} = \frac{\mu}{\bar{p}^g - \underline{p}^g} + \frac{\underline{z}}{2} + \sqrt{(\frac{\mu}{\bar{p}^g - \underline{p}^g})^2 + (\frac{\underline{z}}{2})^2}$
- 6) Recover $\hat{\bar{z}} = \frac{\mu}{\bar{p}^g - \underline{p}^g} - \frac{\underline{z}}{2} + \sqrt{(\frac{\mu}{\bar{p}^g - \underline{p}^g})^2 + (\frac{\underline{z}}{2})^2}$

Note that this procedure is only used during training. During inference, Dual Lagrangian Learning (DLL) [25] is used since it guarantees optimal completion given fixed $\hat{\lambda}$ and $\hat{\pi}$:

- 1) Predict $\hat{\lambda} \in \mathbb{R}$ and $\hat{\pi} \in [-M, M]^E$
- 2) Recover $\underline{\hat{\mu}} = \max(0, \hat{\pi})$.
- 3) Recover $\hat{\bar{\mu}} = \max(0, -\hat{\pi})$.
- 4) Recover $\underline{\hat{z}} = \max(0, c - \hat{\lambda} e - (\Phi A_g)^\top \hat{\pi})$.
- 5) Recover $\hat{\bar{z}} = \max(0, (\Phi A_g)^\top \hat{\pi} + \hat{\lambda} e - c)$.

Note that both the primal and dual recovery procedures require bounded predictions as part of Step 1; the experiments use the “double-softplus” function to enforce the element-wise bound constraints $l \leq x \leq u$ on the neural network predictions: $\tilde{x} := \ln(1 + e^{x-l}) - \ln(1 + e^{x-u}) + l$.

Finally, note that although the hybrid solver framework is applicable for any architecture which produces primal-dual feasible predictions, its performance depends on the inference time of the models, including any repair steps. The procedures described above are chosen due to their computational efficiency, enabling timely training and fast inference.

C. Results

The experiments compare the hybrid solver to the parallelized classical solver described in Section IV-A. For each case, two types of hybrid solvers are evaluated, differing only in the loss function used to train the underlying proxy models: Γ^0 refers to the standard ERM-based loss (7) and $\Gamma^{1\%}$ refers to the “ReLU” loss (10) with a target optimality threshold of $\epsilon=1\%$. All other hyperparameters are kept constant: proxies are trained using the Adam optimizer with batch size 1024 and learning rate $10^{-3} \rightarrow 10^{-5}$, scheduled using the normalized mean duality gap on the validation set. Specifically, the learning rate is multiplied by 0.95 when the gap does not decrease by at least 0.01% for 50 consecutive epochs. The primal and dual proxies each use 4 hidden layers with dimension 256, learned batch-normalization, and softplus activations. Training is run for 5000 epochs with a (re-sampled, as discussed in Section III-C) dataset size of 20,480. Validation is run every epoch using the same 10,240 (unlabeled) samples, and checkpoints are saved based on the best mean normalized duality gap on the validation set. Results are presented on a batch of 240,000 unseen testing samples. This batch size is chosen to mimic performing a 1-day hourly-granularity simulation with 10,000 scenarios.

The training and evaluation is run on an NVIDIA H200 GPU, implemented using PyTorch 2.8.0 [31]. GPU inference uses `torch.compile` including the proxy inference, repair, and objective value calculation. This straightforward inference setup is used to keep the implementation simple; further speedup can likely be achieved by improving this aspect. Furthermore, time spent on data movement (inputs to GPU and outputs to CPU) is *included* in the inference time measurements.

Table II includes the column T_{240k}^{Opt} , reporting the solve time of the perfectly-parallelized classical solver for the test set. The column T_{240k}^{ML} reports the inference time of the proxy

TABLE I
AGGREGATED PERFORMANCE RESULTS ACROSS DIFFERENT WEIGHT INITIALIZATIONS

Case	Loss	100x $\epsilon\%$	500x $\epsilon\%$	1000x $\epsilon\%$	Nx 0.5%	Nx 1%	Nx 2%
1354_pegase	Γ^0	0.43\pm0.01	0.96 \pm 0.17	1.36 \pm 0.20	168.17\pm35.60	588.97 \pm 199.74	1646.03 \pm 199.75
1354_pegase	$\Gamma^{1\%}$	0.65 \pm 0.07	0.75\pm0.08	0.80\pm0.09	1.90 \pm 0.54	1782.84\pm297.92	2163.81\pm2.29
2869_pegase	Γ^0	0.47\pm0.03	1.17 \pm 0.05	1.49 \pm 0.05	109.01\pm6.99	332.89 \pm 26.66	1672.71 \pm 119.89
2869_pegase	$\Gamma^{1\%}$	0.56 \pm 0.04	1.10\pm0.03	1.36\pm0.03	50.27 \pm 34.33	388.00\pm32.21	1798.52\pm19.63
9241_pegase	Γ^0	0.53\pm0.03	0.87 \pm 0.02	2.88 \pm 0.07	82.33\pm18.62	707.22 \pm 57.06	958.89 \pm 18.36
9241_pegase	$\Gamma^{1\%}$	0.57 \pm 0.03	0.85\pm0.04	1.18\pm0.04	64.04 \pm 13.71	925.23\pm39.92	1113.27\pm1.30

TABLE II
CASE SIZES, TIMING STATISTICS, AND PARAMETER COUNTS

Case name	$ p^d $	$ p^g $	$ p^f $	T_{240k}^{Opt}	T_{240k}^{ML}	$T_{\text{Train}}^{\text{ML}}$	$ \alpha + \beta $
1354_pegase	673	260	1991	90.8s	0.03s	28min	1.3M
2869_pegase	1491	510	4582	199.7s	0.09s	32min	2.5M
9241_pegase	4895	1445	16049	711.2s	0.64s	70min	7.4M

models; across all cases, the ML models return predictions for all 240,000 samples in milliseconds, far exceeding the throughput of the parallelized classical solver. The column $T_{\text{Train}}^{\text{ML}}$ shows the training time for the ML models; about 30 minutes for 1354_pegase and 2869_pegase and just over an hour for 9241_pegase. Finally, the $|\alpha|+|\beta|$ column reports the total number of trainable parameters across both the primal and dual models; the largest case uses under 7.5M parameters.

The “ $Nx \epsilon\%$ ” metric is used to analyze the performance of the proposed hybrid solver; it captures at what percent optimality tolerance $\epsilon\%$ the hybrid solver achieves an Nx speedup. In other words, Pareto-optimal hybrid solvers achieve the largest Nx speedups at the lowest $\epsilon\%$ tolerances. Note that, in contrast to NNV-based approaches which only provide a global worst-case bound, the hybrid solver allows practitioners to choose the target optimality threshold $\epsilon\%$, then evaluate the speedup. Table I includes such evaluations for $\epsilon\%=\{0.5\%, 1\%, 2\%\}$, as well as “inverse” results showing at what $\epsilon\%$ level an $N=\{100, 500, 1000\}$ -times speedup is achieved. Furthermore, Figure 1 shows N as a function of ϵ .

Table I shows the hybrid solver performance across cases and when using different training losses for the underlying proxies. Notably, all configurations achieve substantial speedups at practical optimality tolerance levels, all achieving 1000x speedup below 3% tolerance. When using the $\Gamma^{1\%}$ loss configurations, 100x is achieved below 0.7% across all cases and 1000x is achieved below 1.4% for all cases. Furthermore, the difference between the Γ^0 and $\Gamma^{1\%}$ rows highlights the tradeoff associated with targeting an optimality tolerance; speedup for tolerance levels below the target is traded for speedup at and above the target. Notably, $\Gamma^{1\%}$ consistently outperforms Γ^0 at the target tolerance (corresponding to the $Nx 1\%$ column), achieving speedups over 1500x for 1354_pegase, over 350x for 2869_pegase, and over 900x for 9241_pegase. With a higher 2% threshold, speedup is over 1000x for all cases; above 2000x for 1354_pegase.

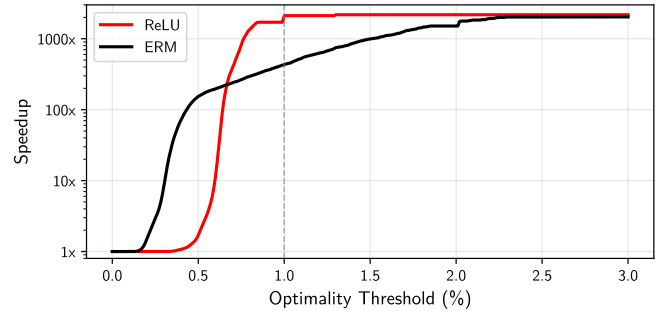


Fig. 1. Speedup of hybrid solver on 1354_pegase as a function of the optimality threshold ϵ .

Figure 1 further explores the impact of using a non-zero target threshold, comparing the speedup-optimality tradeoff curves when using different underlying proxy models, one trained using Γ^0 , labeled ERM, and the other using $\Gamma^{1\%}$, labeled ReLU. The figure shows that, at the 1% target tolerance and above, using the $\Gamma^{1\%}$ models results in larger speedups. At optimality tolerances below the target, Γ^0 begins to outperform $\Gamma^{1\%}$. While $\Gamma^{1\%}$ only achieves 10x speedup for thresholds below 0.6%, Γ^0 achieves over 100x speedup while guaranteeing at most 0.5% sub-optimality.

V. CONCLUSION

This paper has proposed a novel hybrid framework that accelerates large-scale computations in power systems operations and planning by integrating data-driven machine learning proxies and classical optimization solvers in a principled way. The proposed hybrid solver offers substantial speedups and worst-case performance guarantees, thus synergizing several recent developments in machine learning for power systems. This approach further closes the gap between theoretical advances and the tight requirements of practical deployments.

Unlike neural network verification-based approaches, the proposed methodology does not impose strong restrictions on activation functions, does not require any post-training analysis, and provides *adaptable* worst-case optimality guarantees. The paper has conducted extensive computational experiments on large-scale power grids, corresponding to economic dispatch problems with over 10^5 decision variables and constraints, and over 10^4 parameters. Numerical results demon-

strate the scalability of the approach, achieving speedups on the order of 1000x over optimized classical solvers.

ACKNOWLEDGMENTS

This material is based upon work supported by the National Science Foundation under Grant No. 2112533 and Grant No. DGE-2039655, and partially funded by Los Alamos National Laboratory's Directed Research and Development project, "Artificial Intelligence for Mission (ArtIMis)." Any opinions, findings, and conclusions or recommendations expressed in this material are those of the author(s) and do not necessarily reflect the views of the sponsors.

REFERENCES

- [1] Yang Gu and James McCalley. Market-based transmission expansion planning. In *2011 IEEE/PES Power Systems Conference and Exposition*. IEEE, 2011.
- [2] Oliver Stover, Pranav Karve, and Sankaran Mahadevan. Reliability and risk metrics to assess operational adequacy and flexibility of power grids. *Reliability Engineering & System Safety*, 231:109018, 2023.
- [3] Wenbo Chen, Mathieu Tanneau, and Pascal Van Hentenryck. Real-time risk analysis with optimization proxies. *Electric Power Systems Research*, 235:110822, 2024.
- [4] Bernard Knueven et al. Stochastic look-ahead commitment: A case study in MISO. In *2023 IEEE Power & Energy Society General Meeting (PESGM)*. IEEE, 2023.
- [5] Parth Brahmbhatt et al. Benders decomposition using graph modeling and multi-parametric programming. *arXiv:2508.01100*, 2025.
- [6] Hooman Khaloie et al. Review of machine learning techniques for optimal power flow. *SSRN 4681955*, 2024.
- [7] Pascal Van Hentenryck. Trustworthy optimization learning: a brief overview. In *De Gruyter Proceedings in Mathematics*, page 121, 2025.
- [8] Brandon Amos and J Zico Kolter. Optnet: Differentiable optimization as a layer in neural networks. In *International conference on machine learning*. PMLR, 2017.
- [9] Minsoo Kim and Hongseok Kim. Projection-aware deep neural network for dc optimal power flow without constraint violations. In *2022 IEEE SmartGridComm*, pages 116–121, 2022.
- [10] Wenbo Chen et al. End-to-end feasible optimization proxies for large-scale economic dispatch. *IEEE Transactions on Power Systems*, 2023.
- [11] Jesus Tordesillas, Jonathan P How, and Marco Hutter. Rayen: Imposition of hard convex constraints on neural networks. *arXiv:2307.08336*, 2023.
- [12] Youngjae Min and Navid Azizan. Hardnet: Hard-constrained neural networks with universal approximation guarantees. *arXiv:2410.10807*, 2024.
- [13] Gonzalo E Constante-Flores, Hao Chen, and Can Li. Enforcing hard linear constraints in deep learning models with decision rules. *NeurIPS*, 2025.
- [14] Wenbo Chen, Haoruo Zhao, Mathieu Tanneau, and Pascal Van Hentenryck. Compact optimality verification for optimization proxies. In *ICML*, 2024.
- [15] Changliu Liu et al. Algorithms for verifying deep neural networks. *Foundations and Trends® in Optimization*, 2021.
- [16] Rahul Nellikkath and Spyros Chatzivasileiadis. Physics-informed neural networks for minimising worst-case violations in dc optimal power flow. In *2021 IEEE SmartGridComm*, 2021.
- [17] Rahul Nellikkath, Mathieu Tanneau, Pascal Van Hentenryck, and Spyros Chatzivasileiadis. Scalable exact verification of optimization proxies for large-scale optimal power flow. *arXiv:2405.06109*, 2024.
- [18] Shiqi Wang et al. Beta-crown: Efficient bound propagation with per-neuron split constraints for neural network robustness verification. *Advances in neural information processing systems*, 34:29909–29921, 2021.
- [19] Kaijie Xu et al. Explainable warm-start point learning for ac optimal power flow using a novel hybrid stacked ensemble method. *Sustainability*, 2025.
- [20] Wenqian Dong et al. Smart-pgsm: Using neural network to accelerate ac-opf power grid simulation. In *SC20: International Conference for High Performance Computing, Networking, Storage and Analysis*. IEEE, 2020.
- [21] Seonho Park, Wenbo Chen, Terrence WK Mak, and Pascal Van Hentenryck. Compact optimization learning for ac optimal power flow. *IEEE Transactions on Power Systems*, 2023.
- [22] Frederik Diehl. Warm-starting ac optimal power flow with graph neural networks. In *NeurIPS*, 2019.
- [23] Aharon Ben-Tal and Arkadi Nemirovski. *Lectures on modern convex optimization*. SIAM, 2001.
- [24] Panagiotis D Grontas et al. Pinet: Optimizing hard-constrained neural networks with orthogonal projection layers. *arXiv:2508.10480*, 2025.
- [25] Mathieu Tanneau and Pascal Van Hentenryck. Dual lagrangian learning for conic optimization. In *NeurIPS*, 2024.
- [26] Sogol Babaiejadsarookolaee et al. The Power Grid Library for benchmarking AC optimal power flow algorithms. *arXiv:1908.02788*, 2019.
- [27] Michael Klamkin, Mathieu Tanneau, and Pascal Van Hentenryck. PGLearn - an open-source learning toolkit for optimal power flow, 2025.
- [28] Miles Lubin et al. JuMP 1.0: Recent improvements to a modeling language for mathematical optimization. *Mathematical Programming Computation*, 2023.
- [29] Q. Huangfu and J. A. J. Hall. Parallelizing the dual revised simplex method. *Mathematical Programming Computation*, 2018.
- [30] Michael Klamkin, Mathieu Tanneau, and Pascal Van Hentenryck. Dual interior point optimization learning. In *IISE Annual Conference*, 2025.
- [31] Adam Paszke et al. Pytorch: An imperative style, high-performance deep learning library. *NeurIPS*, 2019.